Malaysian Journal of Catalysis
http://mjcat.utm.my/
MJCat Research Article

Synthesis and Characterization of Fe_2O_3/g-C_3N_4 Photocatalyst from Waste Toner Powder

Asmawati @ Fatin Najihah Alias[1], Nur Hazirah Rozali Annuar[2*], Nurul Sahida Hassan[3], Sharifah Najiha Timmiati[4]

[1]*Faculty of Applied Sciences, Universiti Teknologi MARA, Cawangan Johor, Kampus Pasir Gudang, 81750 Masai, Johor, Malaysia.*
[2]*Advanced Biomaterials and Carbon Development, Universiti Teknologi MARA, 40450, Shah Alam, Selangor, Malaysia.*
[3]*Centre of Hydrogen Energy, Institute of Future Energy, Universiti Teknologi Malaysia, 81310 UTM Johor Bahru, Malaysia.*
[4]*Fuel Cell Institute, Universiti Kebangsaan Malaysia, 43600, Bangi, Selangor, Malaysia.*

**Corresponding Author: nurha8558@uitm.edu.my*

Article history:
Received 04 November 2024
Accepted 04 February 2025

ABSTRACT

Modern use of electrical and electronic equipment and the rapid development of technologies lead to the production of electronic waste. Electronic waste management is one of the key challenges for the green revolution without affecting the environment. One of the electronic wastes includes toner powder from the printer. Toner powder consists of polymer, carbon black, Fe_3O_4, additives and charge control agents. This paper focuses on the synthesis and characterization of Fe_2O_3/g-C_3N_4 photocatalyst. Initially, waste toner powder was calcined at 600 °C at air atmosphere to ensure the complete decomposition of organic residues. Then the obtained Fe_2O_3 was mixed with g-C_3N_4 by polycondensation method for fabrication of Fe_2O_3/g-C_3N_4 photocatalyst. The obtained Fe_2O_3, g-C_3N_4 and Fe_2O_3/g-C_3N_4 were characterized by FTIR, SEM, TGA and XRD. FTIR, SEM and XRD results confirm that Fe_2O_3 is successfully incorporated with g-C_3N_4 while TGA analysis demonstrates an excellent thermal stability for Fe_2O_3/g-C_3N_4 photocatalyst. The physicochemical properties of Fe_2O_3/g-C_3N_4 catalyst demonstrated its ability to be utilized in a variety of photocatalytic reactions. Therefore, the utilization of waste toner powder as an iron (Fe) precursor may offer a great opportunity for waste management and the fortification of the environment such as in wastewater treatment.

Keywords: *Electronic waste, Toner powder, Fe_2O_3/g-C_3N_4, Photocatalyst*

| eISSN 0128-2581 |

1. INTRODUCTION

The objectives of the Twelfth Malaysia Plan (12MP) 2021-2025 realigned with the vision of the Ekonomi MADANI relate to the effort for shared prosperity, which encompasses three dimensions: economic empowerment, environmental sustainability, and social re-engineering. Based on the environmental sustainability dimension, it comprises the blue economy, green technology, renewable energy, and climate change adaptation and mitigation [1].

In recent years, to address environmental challenges and promote economic efficiency, there has been a significant increase in interest in the use of waste-derived materials to synthesize advanced photocatalysts. Photocatalytic technology has gained a lot of attention as a potential solution to environmental issues. A photocatalyst is a substrate that absorbs light and acts as a catalyst for chemical reactions, essentially functioning as a semiconductor [2]. Waste-derived can be considered a potentially attractive option for photocatalytic reaction, either utilizing waste as a source of components for photocatalysts such as titanium, sulfur, carbon and Fe or reusing them as catalysts in a synthetic process. To date, electronic wastes such as spent batteries [3], waste printed circuit board [4], waste liquid crystal displays [5], electronic packaging [6], brick waste [7], biomass waste such as soybean [8], lotus seedpod [9], rice husk [10], coffee grounds [11], other agriculture, forestry and food waste have been exploited for the fabrication of photocatalytic materials, absorbent and electrolysis. The conversion of waste as photocatalyst materials is a fascinating option due to its environmentally beneficial, eco-friendly, sustainable technology and green approach [12].

Rapid development in modern technologies, particularly in electrical and electronics and information technology, contributes to producing electronic waste (e-waste). Global e-waste monitor data for 2019 show that only 17.4% of the approximately 53.6 Mt of generated e-waste

was collected and reused [13]. As reported by worldwide e-waste research only about 20% of total world's waste is appropriately handled. The effectiveness of recycling and e-waste disposal are expensive and time consuming compared to profits that might be generated from recycling the electronic waste [14]. To achieve the objective for the e-waste management, a financial system that serves society, procedures and consumers are required [15]. For example, in Asia Pacific countries are facing significance challenges due to lack of policies, infrastructure, and financial resources. Generally, the e-waste recycling step divide into three stages namely as 1) collection, 2) sorting and dismantling and 3) end processing. As for Asia Pacific countries, mostly all the steps are handled by informal recycling sector that shortages in skilled operation which might result in severe environment pollution. To overcome this problem, a strategy that focus on synergising the informal e-waste recycling sector with the formal sector mut be considered. This must include the financial, institutional, political, and social aspects of the country [16]. Besides, the recycling of e-waste also can offer an outstanding business opportunity by converting this e-waste into valuable sources.

Toner-based printing equipment, particularly toner cartridges, is mostly used in the office and printing industries. The quantity of waste toner powder in a used cartridge is about 8% or more depending on the type of printer [17]. The percentage of waste toner was recycled only about 20 – 30% globally and the remaining was disposed via landfilling. Due to its potential health hazard, waste toner was classified as a class 2B carcinogen by World Health Organization (WHO) [17]. The composition of waste toner powder consists of 55.0 wt % polystyrene, 35.0 wt % Fe_3O_4, 7.0 wt % polyacrylate and 3.0 wt % SiO_2, which 62.0 wt % toner waste comprises of organic components that may lead to disease [18]. In recent times, few research has been reported on the recycling of waste toner powder. Waste toner powder was successfully transformed and recycled into valuable materials such as carbon-coated ferric oxides for lithium-ion batteries [19], nano-Fe_3O_4 and nano-SiO_2 for removal of Cr(VI) [20]. Previously, researchers also reported on the reutilization of waste toner powder into 3D graphene oxide [21], TiO_2/Fe_2O_3@nanographite nanohybrid [22] for wastewater treatment and FeO-NC for styrene oxidation [23].

The utilization of waste toner powder as an iron (Fe) precursor can be considered a great opportunity for waste management and the fortification of the environment. Fe_2O_3 was considered as one of the best co-catalyst due to its abundance, stability and matched bond position for efficient charge separation and enhanced photocatalytic activity with TiO_2. Iron oxide can be found as crystal phases of hematite α-Fe_2O_3), maghemite (ν-Fe_2O_3), magnetite ($F_{e3}O_4$), and wustite (FeO). However, the most common iron oxides are Fe_2O_3 and Fe_3O_4. Ferromagnetic Fe_3O_4 was employed with various other compounds in water treatment due to its easy separation of the bulk NPs from aqueous solutions via external magnetic processes or materials. Meanwhile, Fe_2O_3 is widely used in numerous sectors due to its ability to be tailored to precise morphologies, dimension orientation, and structures to produce a chemically and thermodynamically stable oxide. It can also be a good photocatalyst due to its appropriate band gap energy of between 2.0 and 2.2 eV and has high stability in aqueous and simple synthesis and most importantly is the ability to be recycled [22]. According to Khasawneh and Palaniandy, the Fe_2O_3-TiO_3 showed remarkable performance for the removal of persistent organic po llutants (POPs) as well as successful recovery and reusability of the photocatalyst after the treatment process [25]. When hematite is combined with other semiconductors, the visible absorption of the other semiconductor will be increased.

Nowadays, graphitic carbon nitride (g-C_3N_4) catalyst is known as the efficient candidate used to degrade harmful and toxic compounds in the aqueous medium. Its extraordinary properties like high chemical stability, reducibility, low product cost, non-toxicity and tunable band gap (2.7 eV) make it a superior catalyst compared to the others. Nitrogen-rich precursors like thiourea, urea or melamine are thermally polymerized at high temperatures in regulated environments to produce g-C_3N_4. The precursors endure condensation reactions which result in the formation of polymeric structures that are high in carbon and nitrogen. Then, the polymers transformed into g-C_3N_4, a two-dimensional material consisting of hexagonally arranged carbon and nitrogen atoms, upon further annealing at even higher temperatures. The addition of Fe_2O_3 into g-C_3N_4 enhanced the photocatalytic performance under visible light due to the reduction of the recombination rate of photoinduced electron-hole pairs [26]. The presence of Fe_2O_3 allows for efficient charge separation and transfer, while the g-C_3N_4 component provides a high surface area and enhanced light absorption capabilities.

The mixture of carbon-based and other elements found in printer toner, which is typically thrown away after use, can be effectively repurposed to produce value-added products with major environmental benefits. The synthesis of Fe_2O_3/g-C_3N_4 photocatalyst from waste printer toner, on the other hand, may also offer a sustainable method of utilizing important resources for critical environmental applications. In addition, recycling toner powder as iron precursor nanocomposite can eliminate the environmental risks associated with the substantial toner powder waste, thereby fostering a sustainable environment and a circular economy. Therefore, this paper explores the Fe_2O_3/g-C_3N_4 photocatalyst including its preparation method using waste toner powder as an iron precursor via calcination and the synthesized Fe_2O_3/g-C_3N_4 by polycondensation method. Fe_2O_3/g-C_3N_4 photocatalyst was characterized using SEM, FTIR and TGA. Our study aims to understand the physicochemical properties of the photocatalysts and examine their potential uses.

2. EXPERIMENTS

2.1 Synthesis of Fe_2O_3 from Waste Toner Powder

Waste toner powder was obtained from the used toner powder cartridge from Hewlett-Packard printer. The waste toner powder was directly removed from the print cartridge and subsequently, was put into a container for storage purposes. The collected powder was calcined in a muffle furnace for 2 hours at 600 °C in an air atmosphere to obtain Fe_2O_3 and was cooled overnight [27]. The obtained crystalline orange-coloured powder was identified as Fe_2O_3.

2.2 Synthesis of g-C_3N_4 and Fe_2O_3/g-C_3N_4

A 10 g of thiourea purchased from Sigma Adrich was placed in a covered crucible and was heated at 450 °C in a muffle furnace for 2 hours. The calcined thiourea was cooled overnight and the obtained yellow colour product was then ground to a fine powder and designated as g-C_3N_4. For the synthesis of Fe_2O_3-/g-C_3N_4, about 0.25 g of Fe_2O_3 and 4.0 g of thiourea were grounded using a mortar for 15 minutes. The grounded samples then were heated for 2 hours at 450 ℃ in a muffle furnace. Next, the calcined sample was washed using distilled water and dried inside an oven at a temperature of 80 °C for 3 hours [28,29]. As reported by other researchers, thiourea was used as g-C_3N_4 precursor in this experiment due to its rough and porous surface. When the surface is exposed to the light it generates the carrier and as a result, the distance between the carrier and the surface becomes shorter. Then, the recombination process will reduce which promotes a favorable photocatalytic reaction [30].

A

2.3 Catalyst Characterization

The morphology and elements of catalyst materials were investigated using a Scanning Electron Microscope (SEM Jeol JSM, IT200) with a range of magnification for the sample between 1000 to 10000. The functional groups of materials were examined by Fourier transform infrared spectroscopy (Bruker, Vertex 70). Thermogravimetric analysis, TGA (Perkin Elmer, TGA8000) was executed at the temperature between 30 °C to 900 °C at a heating rate of 10 °C/min in the presence of nitrogen gas. The crystal phase of the synthesis catalyst was obtained by XRD (Siemens D5000 diffractometer) operated at 20 mA and 30 kV using Cu Kα radiation (λ = 0.15406 nm) at room temperature.

3. RESULTS AND DISCUSSION

The morphology of catalysts was examined by Scanning Electron Microscopy (SEM) with a magnification of 1000 and 5000 respectively. Figure 1 shows the morphology structure of a waste-derived Fe_2O_3. Based on Figure 1A, the surface structure of Fe_2O_3 shows a surface with a slight unevenness and a little rocky structure. Figure 1B confirms that the structure of the surface seems to be irregular surface with a small spherical shape covering the area [30].

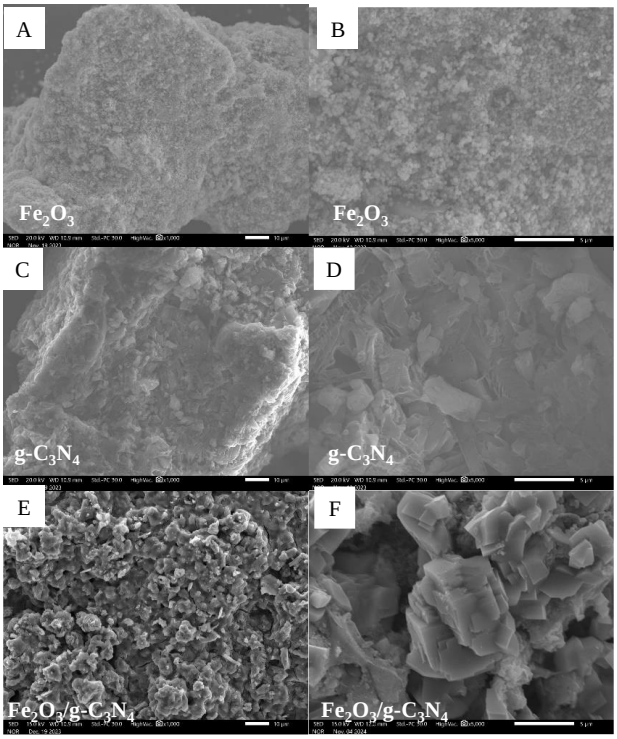

Figure 1. SEM images of Calcined Toner (Fe_2O_3) with a magnification of A) 1000, B) 5000, Calcined Thiourea (g-C_3N_4) with a magnification of D) 1000, E) 5000, and Fe_2O_3/g-C_3N_4 with a magnification of E) 1000, F) 5000

SEM images of g-C_3N_4 derived from thiourea as shown in Figure 1 (C, D) demonstrates the surface of a rocky structure with a large chunk all over the surface. Figure 1D displays the structure of g-C_3N_4 to be an aggregation of rocky particles with uneven size [30]. The microscopic morphology of Fe_2O_3/g-C_3N_4 is also obtained in this analysis. Based on Figure 1E, the surface consists of a rocky structure mixed with spherical-like particles. The surface also shows an unevenness with some areas seeming to be hollow. Figure 3C confirms the combination of Fe_2O_3 and g-C_3N_4 to form Fe_2O_3/g-C_3N_4 as it clearly shows the mixture of rocky and spherical structure shown in Figure 1 [31].

FTIR spectroscopy was utilised to identify the formation and functional groups present in the Fe_2O_3, g-C_3N_4 and Fe_2O_3/g-C_3N_4 as displayed in Figure 2. For Fe_2O_3 catalyst, peak identified at 689 cm^{-1} is attributed to vibration modes of Fe-O, while the peak at 869 cm^{-1} indicates the medium C=C bending [32,33]. An intense absorption peak at 1108 cm^{-1} is assigned to the stretching and bending of Fe-O of -Fe_2O_3 [27]. The bands between 1200 cm^{-1} to 1650 cm^{-1} for g-C_3N_4 and Fe_2O_3/g-C_3N_4 corresponds to the vibrations of C=C, C-N and C-H as reported by Wang et al. [34]. The broad bands ranging from 2900 cm^{-1} to 3400 cm^{-1} are associated to the N-H and O-H stretching vibration [34]. Besides, additional peak appeared at 2920 cm^{-1} can be assigned to Fe-N coordination bond representing an

interface interaction between Fe_2O_3 and g-C_3N_4, which may contribute to the advancement of photocatalytic activity [35]. The FTIR analysis confirms that Fe_2O_3 is successfully incorporated with g-C_3N_4 supported with SEM analysis.

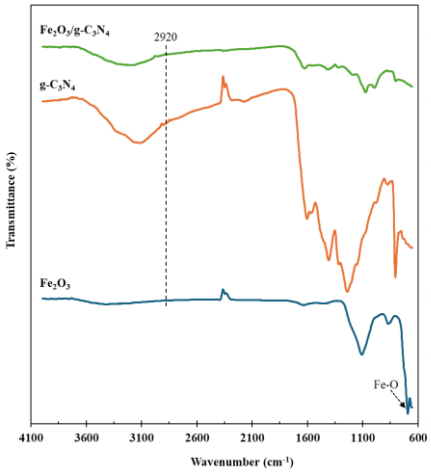

Figure 2. FTIR spectra for Fe_2O_3, g-C_3N_4 and Fe_2O_3/g-C_3N_4 photocatalysts

Thermogravimetric analysis (TGA) was performed to determine the thermal stability and content of organic components in the prepared catalyst. It was conducted under air conditions within the range of 0 to 800 °C. Figure 3A shows the inset of Fe_2O_3 photocatalyst where the weight loss of Fe_2O_3 derived from waste toner powder was slightly decreased to 98.8% due to a low percentage of organic components. The calcination process conducted prior to obtaining Fe_2O_3 removes most of the organic components. For figure 3B, it indicates that the significant weight loss for g-C_3N_4 starts at around 400 °C until the organic components completely decompose at around 700°C. The organic components in Fe_2O_3/g-C_3N_4 catalyst on the other hand starts to decompose around temperature 450°C. At temperature 600°C, maximum rate of decomposition is reached indicates that the catalyst undergoes rapid decomposition and oxidation of g-C_3N_4 and loses about 60% of their initial weight. Babar et al. explained that the decomposition of g-C_3N_4 could be ascribed to the weak van der Waals interactions between conjugated systems in g-C_3N_4 nanosheets caused by Fe_2O_3 particles [27]. At temperatures exceeding 600 °C, Fe_2O_3/g-C_3N_4 demonstrates only insignificant weight loss, implying excellent thermal stability. This divergence delivers valuable understandings into the thermal attributes of these catalysts and provide deeper conception of the role that Fe_2O_3 plays in shaping the behaviour of the photocatalyst.

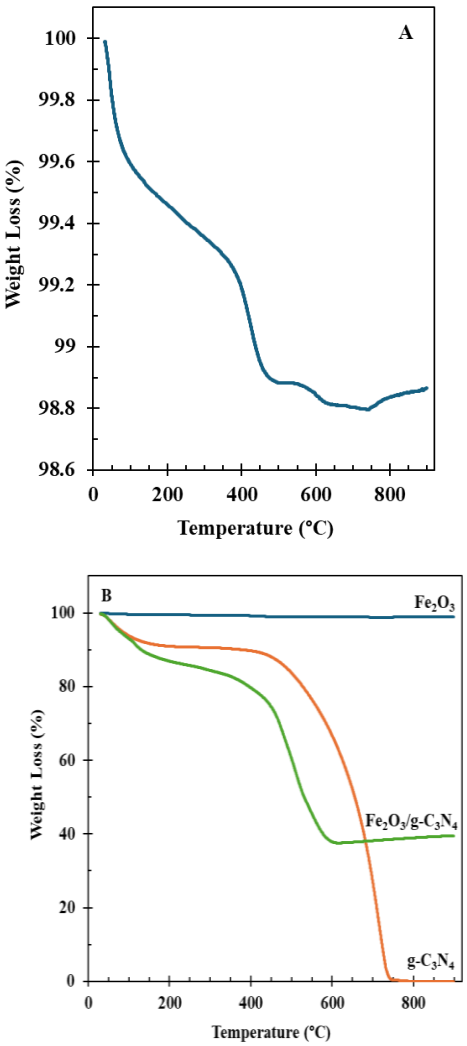

Figure 3. TGA curves of (A) inset of Fe_2O_3 and (B) Fe_2O_3, g-C_3N_4 and Fe_2O_3/g-C_3N_4 photocatalyst

The XRD analysis was carried out to investigate the crystalline structure of the fabricated photocatalyst. The peak of Fe_2O_3, g-C_3N_4 and Fe_2O_3/g-C_3N_4 are shown in Figure 4. The XRD pattern of g-C_3N_4 reveals the presence of hexagonal phase consistent with the standard (JCPDS 87-1526) for graphite-like structure of g-C_3N_4 with a distinct peak at 27.36º belongs to the (002) hkl reflection with a lattice spacing of 0.325 nm due to the interlayer stacking of conjugated aromatic systems [36]. Furthermore, Fe_2O_3 derived from waste toner powder reveals a series of characteristic peaks appeared at 26.36º, 30.43º, 35.79º, 43.54º, 54.09º, 57.42º and 63.09º which correspond to (012), (220), (110), (202), (116), (018) and (214) α-Fe_2O_3 Miller indices (JCPDS card N◦. 33–0664) [27]. The results show that the calcination of waste toner powder at 600 ºC is effective for the phase transformation of α-Fe_2O_3 from Fe_3O_4 and the decomposition of organic residues present in the toner powder [18]. As can be seen from the XRD pattern of Fe_2O_3/g-C_3N_4, adding α-Fe_2O_3 with g-C_3N_4 exhibits the same diffraction pattern as the g-C_3N_4 showing

that the crystal face of Fe_2O_3 successfully incorporates onto g-C_3N_4 with a slight shift of diffraction peak at 27.47° (002). This effect can be explained by the shrinking of the interplanar distance of g-C_3N_4 layers [37]. Meanwhile, the reduction of the intensity of the diffraction peak is due to the presence of Fe_2O_3 deterring the crystal growth of g-C_3N_4 [38]. The characteristics peak relative to α-Fe_2O_3 also can be observed in Fe_2O_3/g-C_3N_4 pattern. Notably, the diffraction peak pattern of Fe_2O_3 has well-resolved compared to Fe_2O_3/g-C_3N_4 with lesser noise. This indicates that the presence of g-C_3N_4 modifies the crystalline properties of α-Fe_2O_3 that might be due to polymeric chain of g-C_3N_4 intrinsic characteristics [39].

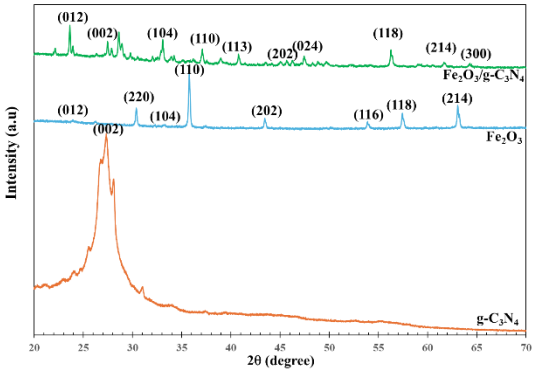

Figure 4. XRD patterns of Fe_2O_3, g-C_3N_4 and Fe_2O_3/g-C_3N_4 photocatalyst

The prepared Fe_2O_3/g-C_3N_4 photocatalyst can be used for the degradation of dye pollution such as methyl orange (MO), methylene blue (MB) and textile effluents (TE). Figure 5 shows the proposed mechanism of photocatalytic degradation using Fe_2O_3/g-C_3N_4 catalyst under sunlight radiation. Fe_2O_3 and g-C_3N_4 could generate electron and hole pairs under visible light irradiation owing to the narrow bandgap [31]. The generated Fe_2O_3 photo electrons migrated to g-C_3N_4 valence band, while the holes retained in conduction band of Fe_2O_3 attributed to the absorption of visible-light which enhanced the photocatalytic activity of the catalyst.

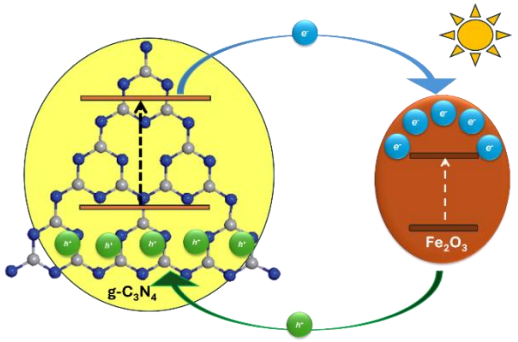

Figure 5. Proposed mechanism of Fe_2O_3/g-C_3N_4 photocatalyst under sunlight radiation

4. CONCLUSION

This study demonstrated a calcination method to transform waste toner powder into Fe_2O_3. The derived Fe_2O_3 was employed to synthesize Fe_2O_3/g-C_3N_4 photocatalyst using thiourea via polycondensation method. SEM, FTIR, TGA and XRD analysis were used to characterize the synthesized catalysts in which SEM images provide visual evidence of the formation of a strongly bonded composite between Fe_2O_3 and g-C_3N_4. Furthermore, the FTIR spectra and XRD analysis showed the existence of functional groups in the catalysts and confirmed a successful incorporation of Fe_2O_3 and g-C_3N_4. For TGA analysis, it depicted that Fe_2O_3/g-C_3N_4 photocatalyst has excellent thermal stability. Hence, Fe_2O_3/g-C_3N_4 photocatalyst derived from ink toner powder can be used as an initial reference for the photocatalytic reaction and industrial applications such as wastewater treatment. This method is cost-effective, safe and sustainable, making it environmentally friendly.

ACKNOWLEDGEMENTS

We would like to thank the School of Chemical Engineering, College of Engineering, Universiti Teknologi MARA, Johor Branch, Pasir Gudang Campus, Malaysia for the access to the instrumentations and facilities.

REFERENCES

[1] Economic Planning Unit (EPU) (2019). Twelfth Malaysia Plan, 2021-2025. Putrajaya.
[2] R. Ameta, M.S. Solanki, S. Benjamin, S.C. Ameta, Photocatalysis. Advanced oxidation processes for wastewater treatment. Academic Press, (2018) 135-175.
[3] W. Zou, X. Feng, W. Wei, Y. Zhou, R. Wang, R. Zheng, J.Li, S. Luo, H.Mi, H.Chen, (2021) 9496–9503.
[4] P. Hadi, J. Barford, G. McKay, (2013) 8248–8255.
[5] C.K. Tsai, R.-a. Doong, H.-Y. Hung, (2019) 337–346.
[6] T.-H. Liou, S.-M. Liu, (2022) 107283.
[7] U.A. Edet, A.O. Ifelebuegu, (2020) 665.
[8] A. Batool, S. Valiyaveettil, (2021) 104902.
[9] N. Liu, Y. Liu, G. Zeng, J. Gong, X. Tan, S. Liu, L. Jiang, Z. Yin, (2020) 10–23.
[10] Z. Wang, J. Yu, X. Zhang, N. Li, B.Liu, Y. Li, Y. Wang, W. Wang, Y. Li, L. Zhang, S. Dissanayake, (2016) 1434-1439.
[11] S. M. Unni., L. George, S.N. Bhange, R. N. Devi, S. Kurungot, (2016) 82103-82111.
[12] D. Rodríguez-Padrón, R. Luque, MJ. Batista. Wste-derived materials: opportunities in photocatalysis. Heterogeneous Photocatalysis: Recent Advances (2020)1-28
[13] V. Forti, C.P. Balde, R. Kuehr, G. Bel, The Global E-Waste Monitor 2020: Quantities, Flows and the

Circular Economy Potential, United Nations University/United Nations Institute for Training and Research, International Telecommunication Union, and International Solid Waste Association, Bonn, Germany; Geneva, Switzerland; Rotterdam, The Netherlands, 2020.
[14] Gregory, J. (2009). E-waste Take-back System Design and Policy Approaches. StEP Initiative, United Nations University.
[15] M. Jain, D. Kumar, J. Chaudhary, S. Kumar, S. Sharma, A. S. Verma, Waste Management Bulletin (2023).
[16] S. Herat, (2021) 45-53.
[16] M. Parthasarathy, (2021) 57.
[17] M. Kouser, B. Chowhan, N. Sharma, M. Gupta, (2022) 47619-47633.
[18] Y. Li, J. Mao, H. Xie, J. Li, (2018) 361–368.
[19] J. Ruan, L. Dong, J. Huang, Z. Huang, K. Huang, H. Dong, T. Zhang, R. Qiu, (2017) 4923–4929.
[20] Z. Tian, L. Sun, H. Tian, K. Cao, S. Bai, J. Li, Q. Zhu, (2021) 5275-5281.
[21] K. Mensah, H. Shokry, M. Elkady, M, H.B. Hawash, M.Samy, (2024) 226-235.
[22] D. Saini, R. Aggarwal, S. R. Anand, N. Satrawala, R. K. Joshi, S. K. Sonkar, (2020) 100256.
[23] C.N.C. Hitam, A. A. Jalil, (2020) 110050.
[24] Khasawneh, O.F.S, P. Puganeshwary,(2021) 101230.
[25] J. Theerthagiri, R. Senthil, A. Priya, J. Madhavan, R. Michael, M. Ashokkumar, (2014) 38222–38229.
[26] S. Babar, N. Gavade, H. Shinde, A. Gore, P. Mahajan, K.H. Lee, V. Bhuse, K. Garadkar, (2019) 103041.
[27] G. Zhang, J. Zhang, M. Zhang, X. Wang, (2012) 8083–8091.
[28] S. Babar, N. Gavade, H. Shinde, P. Mahajan, K.H. Lee, N. Mane, A. Deshmukh, K. Garadkar, V. Bhuse, (2018) 4682–4694.
[29] L.Cao, Y. Li, Z. Zheng, (2022) 1112-1123.
[30] T.J, Al-Musawi, R. Asgariyan, M.Yilmaz, N. Mengelizadeh, A. Asghari, D. Balarak, M. Darvishmotevall, (2022) 137.
[31] L. Wei, X. Zhang, J. Wang, J. Yang, X. Yang, (2024) 111890.
[32] R. Parvari, F. Ghorbani-Shahna, A. Bahrami, S. Azizian, M.J Assari, M. Farhadian, (2020) 112643.
[33] R. Jahanshahi, S. Sobhani, J.M. Sansano, (2020) 10114-10127.
[34] R. Wang, A. Dai, M. Vijayalakshmi, K.R. Reddy, H. Tang, B. Cheolho, J. Shim, C.V. Reddy, (2024) 176086.
[35] Q. Yu, J. Pan, X. Ren, Q. Wang, N. Shi, Y. Li, (2022) 106800.
[36] S. Hmamouchi, A. El Yacoubi, M. El Hezzat, B. Sallek, B. C. El Idrissi, (2024) 100577.
[37] Y. Li, S. Zhu, Y. Liang, Z. Li, S. Wu, C. Chang, Z. Cui, (2020) 109191.
[38] Y. Xu, S. Huang, M. Xie, Y. Li, H. Xu, L. Huang, Q. Zhang, (116) (2015) 95727-35.
[39] T.P. Vijayakumar, M. D. Benoy, J. Duraimurugan, G. S. Kumar, M. Shkir, P. Maadeswaran, R. Srinivasan, S. Prabhu, R. Ramesh, S. Haseena, (2022) 109021.